WATER RESOURCES RESEARCH, VOL. 27, NO. 6, PAGES 995–1003, JUNE 1991

Kinematic Routing Using Finite Elements on a Triangular Irregular Network

DAVID C. GOODRICH, DAVID A. WOOLHISER, AND TIM O. KEEFER

Aridland Watershed Management Research Unit, Agricultural Research Service, U.S. Department of Agriculture Tucson, Arizona

Automated extraction of geometry for hydraulic routing from digital elevation models (DEM) is a procedure that must be easily accomplished for widespread application of distributed hydraulically based rainfall excess–runoff models. One-dimensional kinematic routing on a regular grid DEM is difficult due to flow division and convergence. Two-dimensional kinematic routing on a triangular irregular network (TIN) surmounts many of these difficulties. Because TIN DEMs typically require far fewer points to represent topography than regular grid DEMs, substantial computational economy is also realized. One-dimensional routing using vector contour data overcomes the grid-based routing disadvantages but often requires several orders of magnitude more storage points than a TIN. The methodology presented in this paper represents a compromise between slightly increased computational complexity and the economy of TIN topographic representation. We take the unique approach of subdividing each topographic triangle (TIN facet) into a set of coplanar triangular finite elements, performing routing on a single facet and then routing the resulting excess hydrograph to downstream facets and channels via upstream boundary conditions. Results indicate that shock conditions are readily handled, computed depths match analytic results to within ±3% and volume balances are typically within 1%. This modeling system illustrates the viability of kinematic routing over a TIN DEM derived directly from digital mapping data.

1. INTRODUCTION

Advances in digital mapping have provided hydrologists with a plethora of data products that approximate topographic surfaces. Representation of the watershed surface is of course a key component of any distributed watershed modeling effort. The primary source of topographic information prior to the 1980s consisted of contour maps. Translating this information into geometric elements used in rainfall-runoff calculations is a laborious task. In many cases the topography was distorted into a one-dimensional cascade of planes [*Alley and Smith*, 1982; *Green*, 1984; *Rovey et al.*, 1977; *Kibler and Woolhiser*, 1970; *Woolhiser et al.*, 1990; *Lyngfelt*, 1985; *U.S. Army Corps of Engineers*, 1988] or variable width trapezoid elements [*Ross et al.*, 1977; *Jayawardena and White*, 1979; *Blandford and Meadows*, 1984]. In each of these cases considerable human judgment was required to obtain geometric routing elements. A primary objective of our research effort is to use topographic mapping elements directly as geometric routing elements.

Automatic extraction of geometric routing elements has been made possible by the advent of digital elevation models (DEM). The form of the DEM dictates to a large degree how automation will proceed. The three primary forms of DEM data are regular grid data, triangular irregular networks (TIN), and contour string (vector) data. *Moore et al.* [1988*b*] provide an excellent review of these data types. Regular grid data in digital form are the most commonly available type but algorithms exist to convert various types of DEM data to each of the other forms [*Westwood et al.*, 1984]. From a hydraulic routing viewpoint each type of DEM data also has its particular advantages and disadvantages.

Regular grid data, although computationally convenient, suffer from poor definition of flow paths across grid cells, the inability of objective flow partitioning out of a single cell [*Moore et al.*, 1988*a*], and digital data redundancy in smooth regions. As *Mark* [1978] points out, "the chief source of this (data) structure should be the phenomena in question and not problems, data, or machine considerations as is often the case." As an advantage, regular grid DEMs are easily interfaced with most forms of remotely sensed and raster-based data which are often used to represent soil, vegetation and land use information.

Contour-based data enable the ready definition of stream tubes. Under the assumption that flow does not cross stream tube boundaries, routing computations are easily carried out as a series of one-dimensional coupled equations [*Tisdale et al.*, 1986; *Moore et al.*, 1988*b*]. The chief disadvantage of contour-based data is the large data storage requirement. *Moore et al.* [1988*b*] estimate that approximately one order of magnitude more points are required for comparable surface approximation using contour data than for regular grid data.

In comparing grid and TIN data *Peucker et al.* [1978] and *Mark* [1975] conclude that for varying terrain types from 14 to 250 grid points are required for every TIN point. Two or more orders of magnitude more contour points may therefore be required for surface representation as compared to TIN points if estimates from the previous two references are combined. The efficiencies of TIN DEM data pointed out above result from the "coordinate random, but surface specific" [*Peucker et al.*, 1978] character of a TIN. Because topography is nonstationary [*Pike and Rozema*, 1975] and land use and soil boundaries are irregular, regular grid data must be adjusted to adequately represent the roughest landforms or the small-scale features of soil and landuse. This results in data redundancy in nearby smooth regions. TIN DEMs can be generated to an arbitrary tolerance of slope preservation from regular grid digital elevation models [*Westwood et al.*, 1984]. The resolution of the TIN increases

Paper number 91WR00224.

with a decreasing topographic slope approximation tolerance.

Topographic fit (or slope definition) is one primary parameter that must be defined for routing calculations. Hydraulic roughness is the other primary parameter. If roughness within TIN facets is constant, the economy of TIN surface representation will translate directly into computational routing savings. Should roughness vary within a facet, further subdivision will be required. For infiltration computations, further TIN subdivision is required to acquire homogeneous regions of soil type and land use. Because TIN facets are arbitrarily oriented with respect to the surface gradient, they require a two-dimensional form of the routing equations. This is the primary disadvantage of TIN DEMs for routing computations. This disadvantage is largely mitigated by the methodology presented below.

2. OBJECTIVES

The routing methodology over a TIN DEM described herein represents a compromise between exploiting the economy of the data structure and increased computational complexity of two-dimensional routing. A primary concern in designing our method is automation via the ability to route directly on the TIN DEM as obtained from mapping sources without substantial, and often subjective, DEM data manipulation. With these concerns in mind and the data framework restricted to triangular irregular networks our primary objectives are (1) develop a methodology using two-dimensional kinematic wave equations approximated by finite elements on topographic TIN facets as obtained from mapping sources; (2) test the method against analytic solutions for special cases and route flow across TIN facets boundaries via transformation of boundary conditions; (3) assess the method's ability to handle kinematic shocks; and (4) link the overland flow finite element routing method to a finite difference channel routing scheme to demonstrate the methodology's potential as a watershed rainfall excess routing model. Before formal development of the methodology, background information is presented on prior uses of finite element techniques for watershed routing as well as routing specifically on a TIN DEM.

3. BACKGROUND

3.1. *Finite Element Techniques for Watershed Routing*

TIN facet watershed representation logically leads to finite element methods due to the irregular TIN element shape. In addition to the advantages of finite element techniques over finite difference methods for treating nonrectangular grids, *Raymond and Gardner* [1976] found finite elements to be highly accurate. *Cullen* [1974] also found finite element methods competitive at twice the linear resolution with second-order accurate finite difference schemes when integrating the shallow water equations.

Early work by *Taylor et al.* [1974], *Taylor and Al-Mashidani* [1974], *Taylor* [1976], and *Taylor and Huyakorn* [1978] demonstrated that finite elements could be used on idealized overland flow situations. Solutions were obtained for the St. Venant equations and the simplified kinematic wave (KW) equations. Results of the four previous studies illustrated that when the KW approximation criterion of *Woolhiser and Liggett* [1967] was met virtually no difference existed between KW solutions and those obtained by approximating the St. Venant equations.

Numerous applications to watershed hydrology followed the early works mentioned above. Works by *Aparicio and Berezowsky* [1982], *Ross et al.* [1977, 1979], *Heatwole et al.* [1982], *El-Ansary* [1984], *Judah* [1973], *Judah et al.* [1975], *Jayawardena and White* [1977, 1979], and *Blandford and Meadows* [1984] can be broadly grouped as applications where one-dimensional routing is performed on constant or variable width finite elements. One-dimensional routing on flow strips linked to channels has distinct advantages over multidimensional routing in a computational sense as one-dimensional coupled systems can be used to accomplish routing over a multidimensional surface [*Jayawardena and White*, 1979]. However, from an automation viewpoint, one-dimensional routing schemes suffer the distinct disadvantage of requiring considerable human interpretation (or DEM data processing) to define flow strips and elements.

Taylor and Al-Mashidani [1974] compared full and kinematic wave equations on a simple two-dimensional test case with rectangular finite elements and compared these results to a simple laboratory simulation. The stability of the method was demonstrated but no application to watershed geometries was undertaken. *Kawahara and Yokoyama* [1980] employed the shallow water equations on a regular triangular grid. A large-scale global solution was used and very small time steps were required in their study. Channel routing was not linked into their solution methodology. *Hamrick et al.* [1985] used two-dimensional kinematic wave equations with four-point quadrilateral finite elements in a standard Galerkin formulation and in a streamline upwind modified Galerkin method. Application to a prototype parking lot supplied promising results but linkage to concentrated channel flow was not demonstrated. Although not applied to mapping DEM products, the streamline upwind modified Galerkin method of *Hamrick et al.* [1985] shows potential for application to grid or TIN DEM data if methodology to compute computational order and to handle convergent flow is developed.

Work by *Eraslan et al.* [1981] and *Eraslan and Lin* [1985] is not based on finite elements but on the discrete element method which is conceptually similar to integrated finite differences and uses regular and irregular grid data. Their application derived basin geometry from contour maps, but it appears that regular grid DEM might be easily interfaced with their system.

3.2. *TIN DEM Specific Techniques for Watershed Routing*

Previous work on routing on a TIN has proceeded along two lines. In the first method a TIN facet is converted to an equivalent plane over which one-dimensional routing is performed [*Palacios and Cuevas*, 1989; *Cuevas and Palacios*, 1989; *Silfer et al.*, 1987]. If the TIN facet drains out of two sides, an area-weighted ratio is used to apportion the hydrograph from the equivalent plane to the downstream TIN facets. In the second method, two-dimensional flow equations are used and a global solution is performed over the entire basin TIN network [*Vieux*, 1988].

Vieux [1988] presented a thorough analysis of two-dimensional kinematic wave overland flow routing without

linkage to channel flow. He discusses applications with both linear triangle and four-node quadrilateral elements but found significant shortcomings in the use of both types of elements. These shortcomings limit ready application directly on DEM data. These problems will be discussed in more detail in the section on finite element formulation. However, the primary difficulty with TIN facets is eliminated by using the TIN internal finite element discretization presented below.

4. MATHEMATICAL DEVELOPMENT

The two-dimensional continuity equation for unsteady free surface flow is

$$\frac{\partial h}{\partial t} + \frac{\partial Q_x}{\partial x} + \frac{\partial Q_y}{\partial y} = (q - f) \tag{1}$$

where

h flow depth $[L]$;
t time $[T]$;
Q_x discharge parallel to the x axis $[L^3/TL]$;
Q_y discharge parallel to the y axis $[L^3/TL]$;
q precipitation rate (lateral inflow) $[L^3/TL^2]$;
f infiltration rate (lateral outflow) $[L^3/TL^2]$.

The kinematic wave assumption implies a unique relationship between depth and discharge as

$$Q_x = \alpha_x h^m \tag{2}$$

$$Q_y = \alpha_y h^m \tag{3}$$

where m is the depth-discharge exponent, α_x is the x direction depth-discharge coefficient, and α_y is the y direction depth-discharge coefficient. Uniform flow resistance laws such as Manning's and Chezy's are often utilized to define the coefficients and exponents for (2) and (3). The partial derivatives with respect to x and y in (1) are obtained by differentiating (2) and (3) with respect to x and y, respectively. By substituting the partial derivatives into (1) we obtain

$$\frac{\partial h}{\partial t} + \alpha_x m h^{m-1} \frac{\partial h}{\partial x} + \alpha_y m h^{m-1} \frac{\partial h}{\partial y} = (q - f) \tag{4}$$

The local velocities V_x and V_y are defined as

$$V_x = \alpha_x h^{m-1} \tag{5}$$

$$V_y = \alpha_y h^{m-1} \tag{6}$$

These relations are substituted into (4) to obtain

$$\frac{\partial h}{\partial t} + m V_x \frac{\partial h}{\partial x} + m V_y \frac{\partial h}{\partial y} = (q - f) \tag{7}$$

To address the first objective, (7) is solved over a two-dimensional domain using finite elements to approximate the spatial derivatives. The resulting ordinary differential equations are solved in time via finite differences. Application of the above equations is restricted to those cases for which the kinematic wave approximation is valid [*Woolhiser and Liggett*, 1967]. Routing into pits and routing where backwater effects are significant, such as over microtopography, cannot be treated using the above equations.

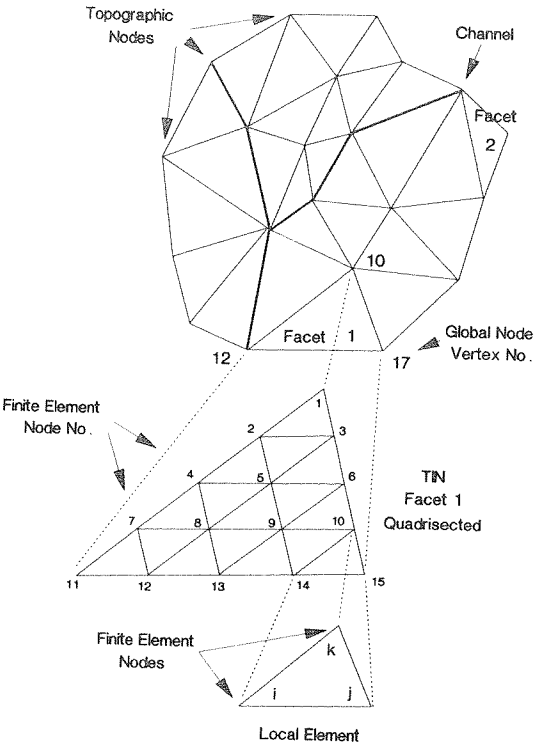

Fig. 1. TIN representation of a hypothetical watershed.

5. FINITE ELEMENT FORMULATION

A triangular irregular network representation of a simple, hypothetical, watershed is illustrated in Figure 1. Each facet has pointers to three nodes, with x, y, and z coordinates, and pointers to adjacent facets. Given this information, *Palacios-Velez and Cuevas-Renaud* [1986], *Maidment et al.* [1989], and *Jones et al.* [1990] have developed methods to extract the drainage network. *Palacios and Cuevas* [1989] have also developed methods to derive the computational order for routing runoff on the TIN facets.

A TIN facet to TIN facet approach is utilized in this study. This is one fundamental difference between the current approach and those of *Vieux* [1988], *Vieux et al.* [1990] and *Kawahara and Yokoyama* [1980], who employed a basin-wide solution of depth and discharge for all triangular finite element nodes at each time step. To accomplish routing on an individual TIN facet, the facet is quadrisected to form 16 local triangular finite elements with the uniform slope of the TIN facet as illustrated in the enlargement of facet 1 in Figure 1. Linear basis functions over the 16 local finite elements are used to approximate the flow depth h on the TIN facet. In this approach the individual TIN facet therefore forms the boundaries of the global solution domain. When using the kinematic wave approximation to the shallow water equations there is no reason to employ a global solution because the nature of the equations does not incorporate the influence of downstream boundary conditions. Routing computations are therefore completed on a facet by facet basis. A complete routing computation (event) begins on a facet along the ridge with a known depth ($h = 0$) upstream boundary condition. Hydrographs are stored at facet outflow nodes so that upstream boundary conditions can then be derived for the routing computation on the next

downstream facet. When a channel is reached, facet outflow becomes lateral inflow for channel routing.

Standard linear basis functions are used to approximate the depth $h(x, y)$ at any location within the facet using the normal linear combination of nodal depths and basis weights as

$$h(x, y) \approx \sum_{i=1}^{n} h_i \Phi_i \tag{8}$$

where

$h(x, y)$ depth within the facet;
h_i nodal depths;
Φ_i linear basis functions;
n number of nodes in a TIN facet (15 for facet quadrisection).

Using linear basis functions the depth at any point in the facet will be approximated by piecewise continuous planar surfaces over the local elements within the facet. Equation (8) is substituted into (7) to form the residual over a local element to obtain

$$\sum_{i=1}^{n} \frac{\partial h_i \Phi_i}{\partial t} + mV_x \frac{\partial h_i \Phi_i}{\partial x} + mV_y \frac{\partial h_i \Phi_i}{\partial y} - (q - f) = 0 \tag{9}$$

In the global assembly over the TIN facet the conventional Galerkin technique is used so the same basis function weights are applied to the local element residuals from (9) to obtain

$$\int_R [\Phi]^T \left[\sum_{i=1}^{n} \frac{\partial h_i \Phi_i}{\partial t} + mV_x \frac{\partial h_i \Phi_i}{\partial x} + mV_y \frac{\partial h_i \Phi_i}{\partial y} - (q - f) \right] dR = 0 \tag{10}$$

where $[\Phi]^T = [\Phi_1, \Phi_2, \cdots, \Phi_n]$ and R is the single TIN facet domain. Upon assembly, (10) may be written in matrix form as

$$[A][\dot{h}] + [B][h] - [C] = 0 \tag{11}$$

Before assembly, further simplification can be achieved if the local coordinates are transformed into a coordinate system in which the surface gradient is parallel to one of the principal axes. This is accomplished by rotating the global coordinate system into a local system with the local y' axis parallel to the surface gradient of the facet before quadrisection (see Figure 2). The following conformal rotation equations are used to rotate (x, y) coordinates of the TIN facet vertex nodes (10, 12, and 17, in Figure 2):

$$\begin{pmatrix} x' \\ y' \end{pmatrix} = \begin{bmatrix} \cos\theta & -\sin\theta \\ \sin\theta & \cos\theta \end{bmatrix} \begin{pmatrix} x \\ y \end{pmatrix} \tag{12}$$

After this rotation all element velocities in the local x direction (V_x) vanish. The resulting one-dimensional system is solved for node depths in a two-dimensional domain and thus the need for two-dimensional elements and basis functions. The rotation is valid because the kinematic wave equations result in a unique correspondence between depth and discharge at a point (see (2) and (3)). Directional discharge differences are only a function of the local roughness, directional components of the surface gradient and excess rainfall rate.

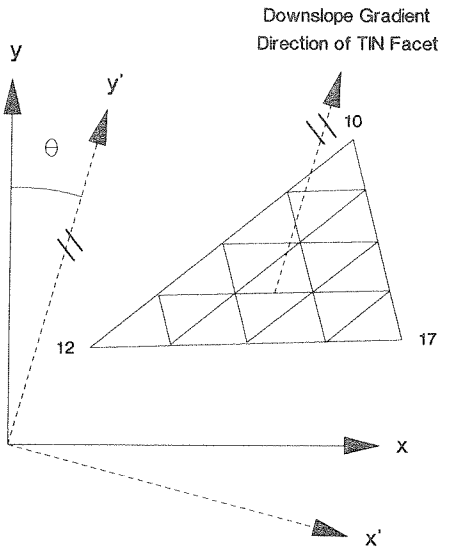

Fig. 2. TIN element and coordinate rotation parallel to slope gradient.

Local coordinate rotation to obtain one-dimensional routing avoids an additional numerical problem encountered by *Vieux* [1988]. Vieux demonstrated that when a four-node quadrilateral finite element is rotated an incompatibility results when integrating to form the $[B]$ matrix. This occurs because the resulting sign and magnitude of elements of $[B]$ are not independent of the ordering used in nodal coordinate assignment to the natural isoparametric coordinate system before Gauss-Legendre quadrature. He recommends against the use of four-node quadrilateral finite elements when anisotropy of slope exists. Further analysis by *Vieux* [1988] showed that triangular elements do not suffer this incompatibility upon rotation and recommends their use. *Vieux* [1988] also found that the most accurate solutions were obtained when one of the finite element sides is parallel to the gradient direction.

After rotation and assembly to form (11) the time derivative of the depth vector is approximated by an ordinary trapezoidal finite difference approximation. The vector of depths at the advance time is obtained using the following equation,

$$[h]^{t+\Delta t} = [D]^{-1}[E][h]^t + \Delta t[D]^{-1}[C] \tag{13}$$

where $[E] = [A] - 0.5(\Delta t)[B]$ and $[D] = [A] + 0.5(\Delta t)[B]$. After rotation the nonzero local element velocities (V_y^e), which contribute to the $[B]$ matrix, are computed from depth values of the local element vertices (h_i, h_j, h_k) at the previous time step (t) as follows:

$$V_y^e = \frac{\alpha_y}{3} [h_i^{m-1} + h_j^{m-1} + h_k^{m-1}] \tag{14}$$

An iterative and a noniterative evaluation of (14) were tested. No significant improvement was found by iterating;

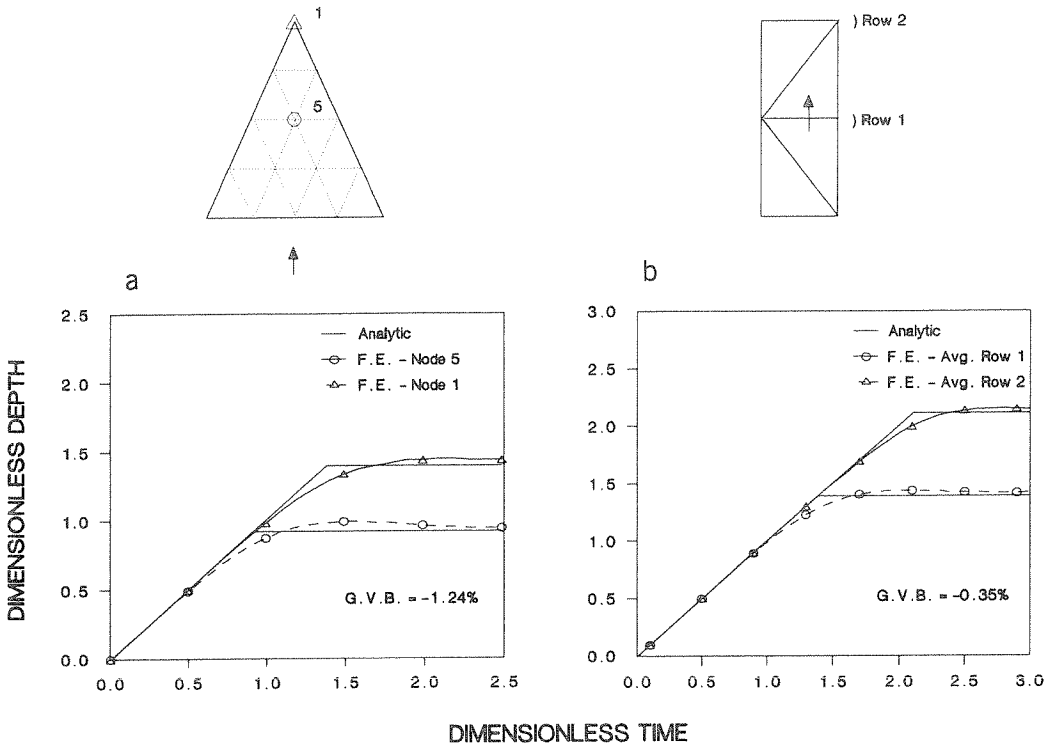

Fig. 3. (*a*) Single and (*b*) four coplanar facet test.

therefore a noniterative approach was employed to further simplify and enhance solution speed.

TIN facet by facet solution of (11) offers several distinct advantages over a basinwide global solution. The system of equations in (11) is small and easily solved. For the level of discretization shown in Figure 1 the maximum number of unknown nodal depths is 10. This condition corresponds to the case where a known upstream boundary condition (inflow or $h = 0$) exists at one edge of the facet and outflow occurs across the remaining two facet edges. For the case where upstream boundary conditions are defined on two facet edges, six unknown nodal depths exist. Because the kinematic wave equations are used, we must exclude the case where flow into the facet occurs on all three boundaries as it would violate basic assumptions. This must be treated in the algorithms which compute the routing sequence over the TIN [*Palacios-Velez and Cuevas-Renaud*, 1986].

Facet by facet routing also allows ready reporting of spatially distributed hydrographs throughout the basin. Finite element discretization within a TIN facet also avoids a problem encountered by *Vieux* [1988] where all three TIN facet nodes (corresponding to nodes of a single finite element in *Vieux*'s [1988] case) fall on the watershed boundary (Figure 1, facet 2). When a global solution over the watershed is used this element has $h = 0$ at all nodes due to the watershed boundary condition and a solution does not exist for it.

To store boundary conditions in the facet to facet routing scheme the nodal depths on the outflow edges of a facet are converted to discharge orthogonal to the facet edge. For each of the five nodes along a facet edge, discharge depths are stored as a function of time. This outflow becomes the upstream boundary condition for the downstream facet. When the downstream facet is being processed, the discharge orthogonal to the boundary is converted back to depth for the slope and roughness of the current facet. If a facet outflow edge contributes to a channel, the facet discharge is treated as spatially variable lateral inflow to the channel segment.

Concentrated flow in a channel segment is routed in a trapezoidal geometry using a one-dimensional, four-point implicit, finite difference method with nine computational nodes. One-dimensional finite differences are used for channel routing because of linear channel segmentation at facet boundaries and assumed uniform channel cross section for each segment. Spatially variable lateral channel inflow is received from adjacent facets. Because spatially variable lateral inflow is received, an analytic solution for the unsteady uniform flow region (zone A) cannot be obtained. This finite difference method is formally described by *Woolhiser et al.* [1990]. However, the implementation described by *Woolhiser et al.* [1990] assumes uniform lateral inflow and incorporates a zone A solution when valid.

6. TESTING AND RESULTS

Several simple noninfiltrating examples were selected for initial testing of the methodology described above. Time step size was selected to meet the criteria of *Woolhiser et al.* [1990] and in each case local (TIN facet) and global (watershed) volume balances were computed for further computational checks. Initial examples included dimensionless, one-dimensional, coplanar cases to allow numerical results to be compared directly to analytic solutions. In Figure 3*a* the numerical finite element solutions at two local facet nodes of a single TIN facet are compared to analytic solutions.

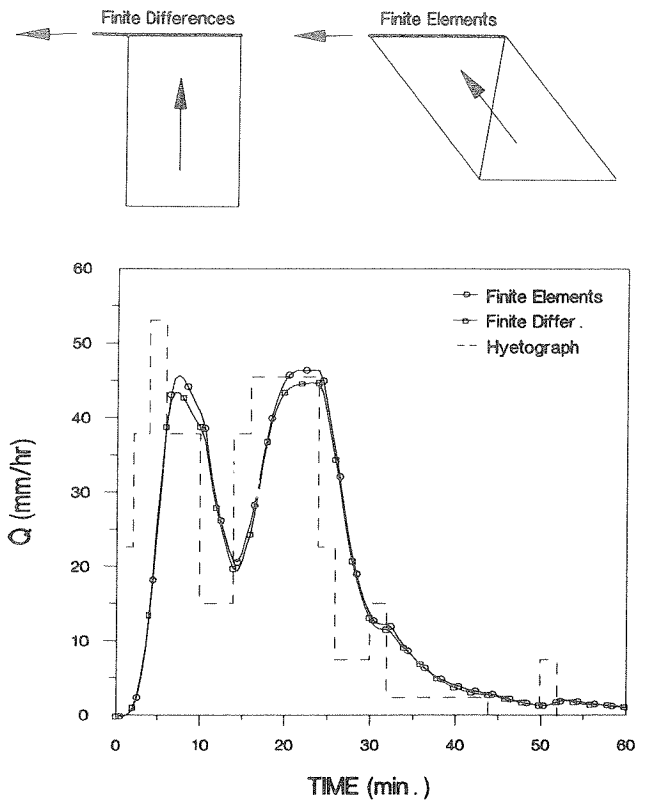

Fig. 4. Comparison of finite element to one-dimensional finite difference solution with channel linkage.

Numerical equilibrium depths for nodes 1 and 5 are within 2.9% and 2.5% of the analytic depths with a local (and global) volume balance error of −1.24%.

The next case, illustrated in Figure 3*b*, was selected to test the ability of the methodology to pass upstream facet solutions across facet boundaries to downstream facets. Four coplanar TIN facets are used in this test. The computed average dimensionless depths of the five local nodes at the end of the second and fourth facet are plotted with the appropriate analytic solutions in Figure 3*b*. Average numerical equilibrium depths for rows 1 and 2 are within 2.2% and 1.4% of the analytic depths and the global volume balance error is −0.35%.

To test linkage of the finite element TIN facet routing to one-dimensional finite difference channel routing the cases illustrated in Figure 4 were employed. In the finite element geometry two coplanar TIN facets are constructed with one-dimensional flow contributing laterally to a single channel element. The response from this case is compared to a finite difference solution obtained from KINEROS [*Woolhiser et al.*, 1990] on a single one-dimensional overland flow plane contributing laterally to a channel. Impervious geometries of each case were constructed with equal area, slope, hydraulic roughness and computational node density in the direction of flow. A rainfall hyetograph from September 13, 1975 of rain gage 384 of the U.S. Department of Agriculture Agricultural Research Service (USDA-ARS) Walnut Gulch experimental watershed was used as input to each of the two systems. The hyetograph and channel outflow hydrographs from the finite element and finite difference solutions are illustrated in Figure 4. Peak outflow rate from the TIN geometry is 3.8% greater than outflow from the KINEROS geometry. Global volume balances from the TIN finite element and KINEROS finite difference solutions were −2.0% and 1.8%, respectively.

In the above cases minor spatial oscillations of computed depth were observed in the finite element solutions over the TIN facets. *Raymond and Gardner* [1976], *Zienkiewicz* [1977], and *Huyakorn and Pinder* [1983], among others, have noted that solutions obtained from the Galerkin method exhibit spatial oscillations for convection-dominated situations. Reduction of the computational grid mesh or using upstream weighting to introduce numerical dispersion are suggested solutions for spurious oscillations. We avoid further discretization as a matter of practicality. Upstream weighting is also not used for several reasons. To obtain an exact solution with upstream weighting the proper weighting coefficient must be selected. However, selection of the coefficient is case dependent [*Zienkiewicz*, 1977]. In addition, upstream weighting is difficult to implement because of the arbitrary orientation of topographic TIN facets in relation to flow direction. *Hamrick et al.* [1985] also found that two-dimensional kinematic wave overland flow solutions obtained from a standard Galerkin method and a streamlined upstream weighting modified Galerkin method were almost identical. For the methodology presented herein further discretization and the implementation of upstream weighting is not warranted due to good agreement with analytic results and reasonable volume balance errors.

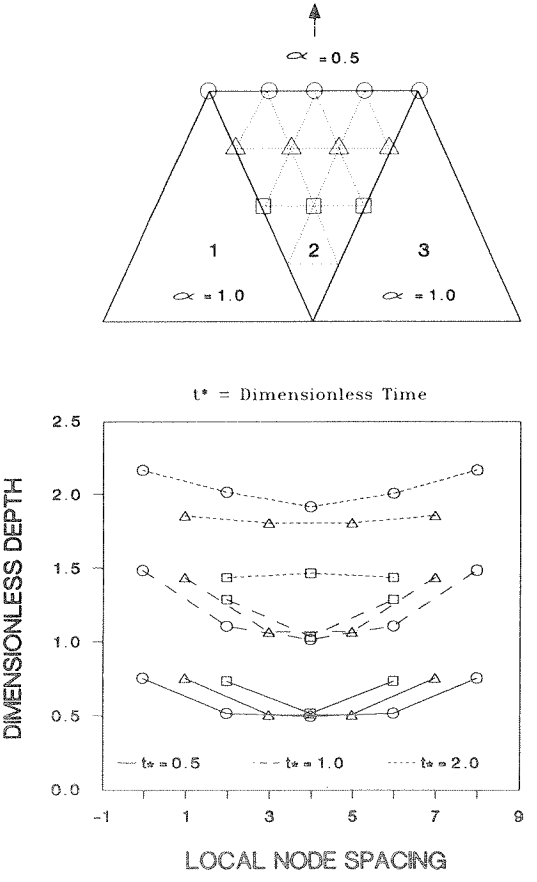

Fig. 5. Cross-gradient dimensionless depth profiles at three times for a kinematic shock condition.

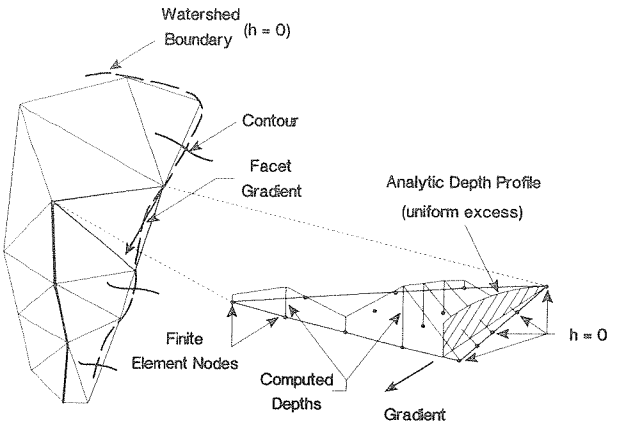

Fig. 6. TIN representation of a portion of the Lucky Hills 106 watershed.

Each of the cases discussed above employed coplanar TIN facets. For a more realistic, noncoplanar condition, kinematic shocks will be encountered where downstream facets have a smaller slope and/or a greater hydraulic roughness. To assess shock handling capability of the TIN facet finite element methodology the case shown in Figure 5 was constructed. For a uniform pulse of rainfall, dimensionless depth profiles across TIN facet 2 are shown at three dimensionless times. The local volume balance error for TIN facet 2 is 0.10% and the global volume balance error for the three-facet system is 0.24%. This case illustrates the progression of the shock into the interior of TIN facet 2 and demonstrates the ability of the numerical methodology to adequately treat a shock condition.

In a final test, the TIN routing methodology was applied to the topography of a portion of the Lucky Hills 106 catchment consisting of 15 facets and three channels (see Figure 6). This catchment is a subbasin of the USDA-ARS Walnut Gulch Experimental Watershed. While testing the method on this catchment a problem was encountered. The problem occurs when a TIN gradient direction is nearly parallel to a facet edge which is a watershed flow line boundary. This condition can occur due to the inexact TIN approximation of the topography (see Figure 6). If this condition occurs, analytical results predict development of a depth profile along the gradient direction for constant excess rainfall. However, the current algorithm implementation assigns the TIN facet edge along the watershed boundary to a zero depth boundary condition. To maintain volume balance the finite element algorithm forces the row of local nodes adjacent to the facet edge to have artificially larger depths. This induces an oscillation which can force nodes to have a negative, erroneous, depth (see Figure 6). The zero depth boundary condition is too stringent in this case and other boundary conditions will be investigated in future efforts to address this problem.

However, this problem can be avoided if the gradient is parallel to the TIN facet edge, implying a proper TIN approximation of the topography. In this case the depth on the nodes of the facet edge is not set to zero and the runoff depth profile develops normally in a downstream direction along the flow line. To insure gradient alignment with a TIN facet flow line boundary it is envisioned that the algorithms of *Palacios-Velez and Cuevas-Renaud* [1986], *Palacios and Cuevas* [1989], and *Jones et al.* [1990] can be modified to automatically detect and correct facet flow line edge and gradient alignment. For the partial Lucky Hills 106 case tested above, manual adjustments to TIN vertex locations were made and routing was successfully completed. The response from this case is compared to a one-dimensional finite difference solution on overland flow planes and channels obtained from KINEROS [*Woolhiser et al.*, 1990] in Figure 7. The KINEROS representation had three channel elements and six overland flow planes. Comparisons are shown for both a simple rainfall excess pulse and for the same rainfall event used in Figure 4. Global volume balances from the TIN finite element and finite difference solutions were −2.4% and 0.05% for the excess pulse and −2.1% and 0.47% for the rainfall event, respectively. The similarity of results between the two models (Figure 7) is not unexpected. Because a common topographic map was used to construct both the KINEROS and TIN facet representations the resulting slope distributions for the two models were very similar. In addition, a common hydraulic roughness was used for both models.

The computational requirements for the finite element routing method are more intensive than a one-dimensional

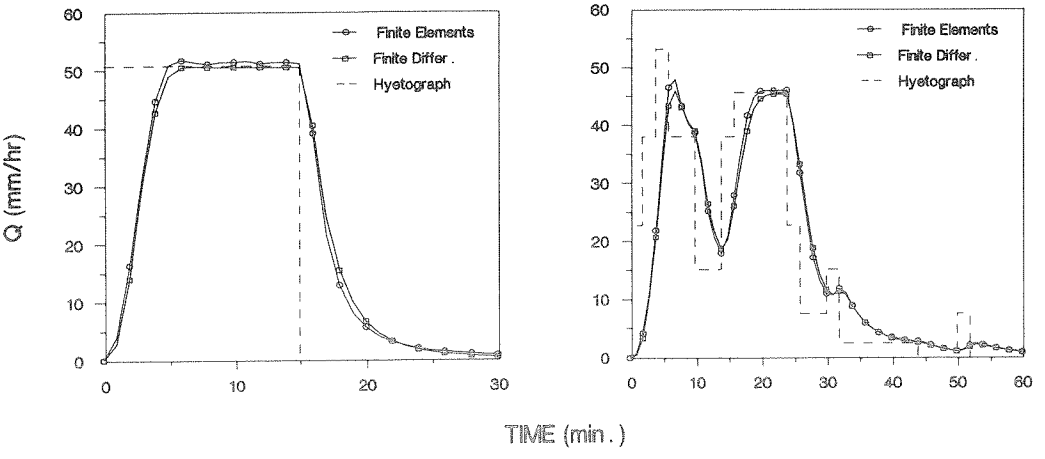

Fig. 7. Comparison of finite element to one-dimensional finite difference solution on Lucky Hills for two excess input cases.

TABLE 1. Computational Time Comparison Between Finite Element and One-Dimensional Finite Difference Solutions for Several Equivalent Geometries

	Finite Element		One-Dimensional Finite Difference	
	Number of Facets	CPU Time, s	Number of Overland Flow Planes	CPU Time, s
Case 1	4	28	2	9
Case 2	6	44	3	13
Case 3	15	88	11	16

finite difference routing scheme. This is illustrated in Table 1 where the CPU time (VAX 11/750) for the two schemes is compared for equivalent basin geometries and excess rainfall hyetographs. Although the finite element computational time requirements are greater it must be kept in mind that considerable interpretive time must be expended to derive the overland flow plane geometries for one-dimensional finite difference routing. From experience, it is the authors' opinion that the advantages of objective automatic derivation of routing geometry directly from TIN mapping products and subsequent finite element routing outweigh the added computational burden.

7. Conclusions

The local TIN finite element routing strategy was tested to illustrate the viability of the method for kinematic routing of excess rainfall on small catchments. The technique capitalizes on the coordinate random, surface specific efficiency of a triangular irregular network of digital elevation data to represent topography. Quadrisection of individual TIN facets and local coordinate rotation orthogonal to the surface gradient permits ease of application by providing a small system of simultaneous equations for solution. The technique also possesses sufficient numerical robustness to handle kinematic shocks. Facet by facet routing also allows ready incorporation of one-dimensional, finite difference, channel routing. The results indicate that further research to incorporate infiltration and additional refinement of numerical techniques is warranted. Comparisons of this routing technique with techniques based on contour and regular grid DEM data will also be conducted as part of future research.

Acknowledgments. The authors express their sincere appreciation to Gordon Wittmeyer at the University of Arizona, A. J. Baker at the University of Tennessee and Tim J. Baker of Princeton University for their encouraging and helpful suggestions and comments. Two anonymous reviewers are also acknowledged for their helpful suggestions.

References

Alley, W. M., and P. E. Smith, Distributed routing rainfall-runoff model—Version II, user's manual, *USGS-WRD Open-File Rep. 82-344*, Gulf Coast Hydrosci. Cent., NSTL Station, Miss., 1982.

Aparicio, F. J., and M. Berezowsky, A distributed rainfall-runoff model, in *Finite Elements in Water Resources*, pp. 4-3 to 4-12, Springer-Verlag, New York, 1982.

Blandford, G. E., and M. E. Meadows, Finite element simulation of kinematic surface runoff, in *Finite Elements in Water Resources, Proceedings, 5th International Conference, Comput. Mech. Cent. Publ.*, pp. 153–164, Springer-Verlag, New York, 1984.

Cuevas, B., and O. L. Palacios, SHIFT: A distributed runoff model using irregular triangular facets (abstract), *Eos Trans. AGU*, *70*(43), 1094, 1989.

Cullen, M. J. P., A finite-element method for a non-linear initial value problem. *J. Inst. Math. Its Appl.*, 13, 233–247, 1974.

El-Ansary, A. S. E., Application of a finite element model to overland and channel flow in arid areas. M.S. thesis, 81 pp., Dep. of Civ. Eng., Univ. of Ariz., Tucson, 1984.

Eraslan, A. H., and W. L. Lin, Application of discrete-element computational models to transient, multi-dimensional problems in hydrology, paper presented at Special Conference on Hydraulics and Hydrology in the Small Computer Age, Hydraul. Div., Am. Soc. of Civ. Eng., Lake Buena Vista, Fla., Aug. 12–17, 1985.

Eraslan, A. H., I. H. Ismail, and W. L. Lin, A fast-transient, two-dimensional, discrete-element rainfall-runoff model for channelized, composite subsurface-surface flows in valleys with steep terrain, in *Applied Modeling in Catchment Hydrology*, edited by V. P. Singh, pp. 3–48, Water Resources Publications, Fort Collins, Colo., 1981.

Green, I. R. A., WITWAT stormwater drainage program: Version II *Rep. 2*, Dep. Civ. Eng., Univ. of the Witwatersrand, Johannesburg, Republ. of South Afr., 1984.

Hamrick, J. M., T. S. Tisdale, and S. L. Yu, Numerical models for two-dimensional surface runoff, paper presented at Special Conference on Hydraulics and Hydrology in the Small Computer Age, Hydraul. Div., Am. Soc. of Civ. Eng., Lake Buena Vista, Fla., Aug. 12–17, 1985.

Heatwole, C. D., V. O. Shanholtz, and B. B. Ross, Finite element model to describe overland flow on an infiltrating watershed, *Trans. ASAE, 25SW*, 630–637, 1982.

Huyakorn, P. S., and G. F. Pinder, *Computational Methods in Subsurface Flow*, pp. 206–212, Academic, San Diego, Calif., 1983.

Jayawardena, A. W., and J. K. White, A finite element distributed catchment model, I, Analytical basis, *J. Hydrol.*, *34*, 269–286, 1977.

Jayawardena, A. W., and J. K. White, A finite element distributed catchment model, II, Application to real catchments. *J. Hydrol.*, *42*, 231–249, 1979.

Jones, N. L., S. G. Wright, and D. R. Maidment, Watershed delineation with triangle-based terrain models, *J. Hydraul. Div. Am. Soc. Civ. Eng.*, *116*(10), 1232–1251, 1990.

Judah, O. M., Simulation of runoff hydrographs from natural watersheds by finite element method, Ph.D. thesis, Va. Polytech. Inst. and State Univ., Blacksburg, 1973.

Judah, O. M., V. O. Shanholtz, and D. N. Contractor, Finite element simulation of flood hyrographs, *Trans. ASAE, 18SW*, 518–522, 1975.

Kawahara, M., and T. Yokoyama, Finite element method for direct runoff flow, *J. Hydraul. Div. Am. Soc. Civ. Eng.*, *106*(HY4), 519–534, 1980.

Kibler, D. F., and D. A. Woolhiser, The kinematic cascade as a hydrologic model, *Hydrol. Pap. 39*, 27 pp., Colo. State Univ., Fort Collins, 1970.

Lyngfelt, S., On urban runoff modeling: The application of numerical models based on the kinematic wave theory, *Rep. Ser. A:13*, vol. 1, Dep. of Hydraul., Chalmers Univ. of Technol., Göteborg, Sweden, 1985.

Maidment, D. R., D. Djokic, and K. G. Lawrence, Hydrologic modeling on a triangulated irregular network (abstract), *Eos Trans. AGU*, *70*(43), 1091, 1989.

Mark, D. M., Computer analysis of topography: A comparison of terrain storage methods, *Geograf. Ann.*, *57A*, 179–188, 1975.

Mark, D. M., Concepts of "data structure" for digital terrain models, paper presented at Symposium on DTMs, Am. Soc. of

Photogramm./Am. Congr. of Surv. and Mapp., St. Louis, Mo., 1978.

Moore, I. D., E. M. O'Loughlin, and G. J. Burch, A contour based topographic model for hydrological and ecological application, *Earth Surf. Processes Landforms*, *13*(4), 305–320, 1988*a*.

Moore, I. D., J. C. Panuska, R. B. Grayson, and K. P. Srivastava, Application of digital topographic modeling in hydrology, Proceedings of International Symposium on Modeling Agricultural, Forest, and Rangeland Hydrology, *Publ. 07-88*, pp. 447–461, Am. Soc. of Agric. Eng., St. Joseph, Mich., 1988*b*.

Palacios, O. L., and B. Cuevas, Transformation of TIN DEM data into a kinematic cascade (abstract), *Eos Trans. AGU*, *70*(43), 1091, 1989.

Palacios-Velez, O. L., and B. Cuevas-Renaud, Automated river-course, ridge and basin delineation from digital elevation data, *J. Hydrol.*, *86*, 299–314, 1986.

Peucker, T. K., R. J. Fowler, J. J. Little, and D. M. Mark, The triangulated irregular network, paper presented at Symposium on DTMs, Am. Soc. of Photogramm./Am. Congr. of Surv. and Mapp., St. Louis, Mo., 1978.

Pike, R. J., and W. J. Rozema, Spectral analysis of landforms, *Ann. Assoc. Am. Geogr.*, *65*(4), 499–516, 1975.

Raymond, W. H., and A. Gardner, Selective damping in a Galerkin method for solving wave problems with variable grids, *Mon. Weather Rev.*, *104*, 1583–1590, 1976.

Ross, B. B., D. N. Contractor, and V. O. Shanholtz, Finite element simulation of overland and channel flow, *Trans. ASAE*, *20*(4), 705–712, 1977.

Ross, B. B., D. N. Contractor, and V. O. Shanholtz, A finite-element model of overland and channel flow for assessing the hydrologic impact of land-use change, *J. Hydrol.*, *41*, 11–30, 1979.

Rovey, E. W., D. A. Woolhiser, and R. E. Smith, A distributed kinematic model of upland watersheds, *Hydrol. Pap. 93*, 52 pp., Colo. State Univ., Fort Collins, 1977.

Silfer, A. T., J. M. Hassett, and G. J. Kinn, Hydrologic runoff modeling of small watershed: The TINFLOW model, paper presented at Engineering Hydrology Symposium, Hydraul. Div. Am. Soc. of Civ. Eng., Williamsburg, Va., Aug. 3–7, 1987.

Taylor, C., A computer simulation of direct runoff, in *Proceedings of First International Conference on Finite Elements in Water Resources*, pp. 4.149–4.163, Pentech, London, 1976.

Taylor, C., and G. Al-Mashidani, An analysis of two-dimensional surface runoff by finite elements, paper presented at International Conference on Computer Methods in Nonlinear Mechanics, Natl. Sci. Found., Austin, Tex., Sept. 23–25, 1974.

Taylor, C., and P. S. Huyakorn, A comparison of finite element based solution schemes for depicting overland flow, *Appl. Math. Modell.*, *1978*(2), 185–190, 1978.

Taylor, C., G. Al-Mashidani, and J. M. Davis, A finite element approach to watershed runoff, *J. Hydrol.*, *21*, 231–246, 1974.

Tisdale, T. S., J. M. Hamrick, and S. L. Yu, Kinematic wave analysis of overland flow using topography fitted coordinates (abstract), *Eos Trans. AGU*, *67*(16), 271, 1986.

U.S. Army Corps of Engineers, HEC-1 flood hydrograph package computer program, Hydrol. Eng. Cent., Davis, Calif., 1988.

Vieux, B. E., Finite element analysis of hydrologic response areas using geographic information systems, Ph.D. dissertation, 199 pp., Mich. State Univ., East Lansing, 1988.

Vieux, B. E., V. F. Bralts, L. J. Segerlind, and R. B. Wallace, Finite element watershed modeling: One-dimensional elements, *J. Water Resour. Plann. Manage. Div. Am. Soc. Civ. Eng.*, in press, 1990.

Westwood, I. J., K. P. Holz, and R. Ratke, On the application of digital surface representations in hydrodynamic modeling, in *Finite Elements in Water Resources, Proceedings, 5th International Conference, Comput. Mech. Cent. Publ.*, pp. 521–531, Springer-Verlag, New York, 1984.

Woolhiser, D. A., and J. A. Liggett, Unsteady one-dimensional flow over a plane—The rising hydrograph, *Water Resour. Res.*, *3*(3), 753–771, 1967.

Woolhiser, D. A., R. E. Smith, and D. C. Goodrich, KINEROS, A kinematic runoff and erosion model: Documentation and user manual, *Rep. ARS-77*, 130 pp., Agric. Res. Serv., U.S. Dep. of Agric., Washington, D. C., 1990.

Zienkiewicz, O. C., *The Finite Element Method*, pp. 633–639, McGraw-Hill, New York, 1977.

D. C. Goodrich, T. O. Keefer, and D. A. Woolhiser, USDA Agricultural Research Service, Aridland Watershed Management Research Unit, 2000 East Allen Road, Tucson, AZ 85719.

(Received October 16, 1990;
revised December 26, 1990;
accepted January 17, 1991.)